Measurement 46 (2013) 4282–4292

Contents lists available at ScienceDirect

Measurement

journal homepage: www.elsevier.com/locate/measurement

Talkha steel highway bridge monitoring and movement identification using RTK-GPS technique

Mohamed T. Elnabwy [a,c], Mosbeh R. Kaloop [b,*], Emad Elbeltagi [a,1]

[a] Structural Engineering Department, Faculty of Engineering, Mansoura University, Mansoura 35516, Egypt
[b] Public Works Engineering Department, Faculty of Engineering, Mansoura University, Mansoura 35516, Egypt
[c] Survey Research Institute, National Water Research Center, Giza 1211, Egypt

ARTICLE INFO

Article history:
Received 21 January 2013
Received in revised form 3 August 2013
Accepted 6 August 2013
Available online 27 August 2013

Keywords:
Bridge
GPS
Monitoring
Structural health monitoring
NNAR model

ABSTRACT

Monitoring the bridge deformation is the vital task in bridge maintenance and management. Talkha highway steel bridge is one of the two oldest steel bridges in Mansoura city. Nowadays, the Real Time Kinematic-Global Positioning System (RTK-GPS) is capable of providing fast and accurate measurements of bridge oscillations. Also, the movement and damage severity can be identified using the dynamic bridge characteristics obtained from GPS. The aim of the present work is to demonstrate the use of RTK-GPS (1 Hz) to provide data for use in the assessment of existing structures. The moving average filter is used to de-noising the GPS observations. Finite Impulse Response (FIR) with moving average are used to extract the dynamic response and frequency domain of the bridge and Neural Network Auto-Regressive (NNAR) model is used to identify the bridge movement. The results indicate that: (1) the moving average filter is simple and suitable to smooth high noises and errors of GPS observation signals; (2) the multi-filter of short-period can reveal the dynamic displacement of bridge deck movement; (3) the low-frequency movements of the bridge could not be completed and the observation time should be increased to complete it and (4) the movement output of the NNAR is highly conformed with the observation filter.

1. Introduction

Bridges are vital links in road infrastructure networks and it is important to keep them well maintained, despite their difficult operating conditions. So, monitoring bridges deformation is the vital task in bridge maintenance and management. The bridge monitoring system is responsible for the reliable collection of response data measured using sensors installed in the bridge members. Once data are collected by the monitoring system, bridge members' deformation and damage detection algorithms are necessary to automate the task of interrogating the data for signs of structural distress and deterioration [1–3]. The process of implementing a movement and damage identification strategy for civil and mechanical engineering infrastructure is referred to as Structural Health Monitoring (SHM) [2]. In addition, SHM is to improve the safety and reliability of structures by detecting damage before it reaches a critical state [4].

The applications of the SHM system to bridges are greater widespread compared with numerous case studies and successful implementations and operations of SHM to other structures [1,2]. Because of their slender geometry, bridges can be significantly affected by wind, vehicle, and other impact loads. Bridges may, also, suffer from large deformations due to temperature changes. Thus, bridges have to be continuously assessed by appropriate monitoring methods to secure their structural performance. All dynamic SHM implementations rely on data, measured with

* Corresponding author. Tel.: +20 050 2244403; fax: +20 050 2244690.
E-mail addresses: eng.elnabwy@yahoo.com (M.T. Elnabwy), mosbeh.kaloop@gmail.com (M.R. Kaloop), eelbelta@mans.edu.eg (E. Elbeltagi).
[1] Tel.: +20 050 2244403; fax: +20 050 2244690.

0263-2241/$ - see front matter Crown Copyright © 2013 Published by Elsevier Ltd. All rights reserved.
http://dx.doi.org/10.1016/j.measurement.2013.08.014

a suitable sampling rate, acquired by a certain number of sensors mounted on the structure to be monitored. The measures obtained from these sensors are the structure response to external or internal mechanical excitations due to wind and other meteorological phenomena, vehicle traffic, seismic events, mass movements [5,6] or use of specific excitation hardware like mechanical shaker [5]. The state of the structure can be evaluated by comparing the responses obtained in reference conditions with the current ones. These comparisons could be (and, sometimes, are) performed by directly extracting from the collected time series information depending only on the structure, for instance their power spectra. A simpler method for the determination of the dynamic characteristics of structures is through the use of ambient vibration measurements [6]. In output-only characterization, the ambient response of a structure is recorded during ambient influence (i.e. without artificial excitation) by means of highly-sensitive velocity or acceleration sensing transducers [6].

Conventional monitoring methods have been employed using accelerometer, tilt meters, strain gauges, (laser) optical devices and survey equipment [7–12]. The accelerometer monitoring system is capable of measuring the dynamic response of structures; while the survey monitoring methods can be employed for measuring the static response [7,8]. Some newly developed techniques, such as robotic total station and terrestrial microwave interferometry systems, laser displacement sensors and photo/video imaging methods have been applied to monitoring of structures with some limitation [8–11]. Unlike other sensors, the use of Global Positioning System (GPS) is readily able to provide three-dimensional absolute position information at a rate of 20 Hz, and higher rates if necessary [13]. Hence providing an opportunity to monitor the dynamic characteristics of the structure to which GPS antenna is attached, also the rapid advancement of the GPS device and algorithms has enabled the monitoring of bridges in continuous real-time, that is commonly referred to as real-time kinematic (RTK) [8–11,13]. The RTK-GPS is now actively applied to measure static, quasi-static and dynamic displacement responses of a large civil engineering structure under different loads due to its global coverage and continuous operation under all meteorological conditions [14]. This enables the analysis of the frequency response and (by using multiple receivers in strategic locations) the dynamics of the vertical profile [15]. Attempts have also been made to use RTK-GPS alone to monitor very long span suspension bridges due to the shortcomings of using an accelerometer to measure slow structural movement with a vibration frequency lower than 0.2 Hz [16]. In the last years, a large number of measurements of structures displacements using RTK-GPS has been published (for review, see [8,14]), and these data open a new era for SHM.

Time-series analysis takes into account the fact that data points taken over time have an internal structure such as: autocorrelation, trend or seasonal variation [4,17]. The system models can be simulating the time series of the output quantities. The models are then expressed as the relationship between the selected system inputs and outputs. In SHM, the identification model can be used as a damage-sensitive feature extractor based on two approaches [4]: (1) using the identification parameters; and (2) using the residual errors. The first approach consists of fitting an identical model to signals from undamaged and damaged structures. Then, the identification parameters are used as a damage-sensitive features. The second approach consists of using the identification model, with parameters estimated from the baseline condition, to predict the response of data obtained from a potentially damaged structure [18,19]. Normally the statistical tests were used to detect the changes in the time series [4,20]. The neural network can be incorporated into the filtering mechanism as a dynamic model corrector for identifying the real-time nonlinear dynamic errors when uncertainty modeling is considered [21,22]. Jwo et al. [22] stated that the applications of the neural network aided adaptive Kalman filter should be introduced to the GPS navigation and receiver tracking loop design.

This paper aims to demonstrate the use of RTK-GPS to provide data for use in the experimental assessment of existing structures. Also, it investigates the use of GPS receivers in measuring the system response of the Talkha highway steel bridge and the nature of its dynamic deformations. In addition, this paper focuses on studying the bridge movement model identification based on RTK-GPS observations.

2. Bridge description, data collection and primary analysis

Talkha highway steel bridge (Fig. 1c) is one of the two oldest steel bridges in Mansoura city, the bridge consists of five-spans and has total length of 230.0 m and width of 20.75 m (Fig. 1a and d) – it has two vehicle lanes for traffic on each direction and two pedestrian walkways. The bridge crosses Damietta River Nile branch, linking Mansoura city (P3) to Talkha city (P4), as shown in (Fig. 1a). The bridge was designed and constructed from 1951 to 1953 by a German Company (Dortmunder Union). This bridge is a main connection between P3 and P4, whereas in one hour at least 4000 vehicles are passing on this bridge. As shown in Fig. 1d, the bridge contains three parts: the first part is a simple supported truss (50.0 m); the second part is a continuous two-spans truss (30.0 m each) and this part is moved to cantilever supported in case of opening the ship way of the river and the third part is two-spans continuous truss (50.0 and 70.0 m). In 1991, the bridge is closed because of un-normal movement on the third part of the bridge. Accordingly, this part was stiffened by adding a new bracing system for the bridge deck of this part.

The data analysis in the present paper obtained through using a GPS (rover) receiver clamped at the mid-span (points C1 and C2) of the third part and another one (point C3) at the intermediate support of this part. All points are located on the top of the handrail of the sidewalk of the bridge, as shown on Fig. 1d. The measurement system is a real time kinematic (RTK) GPS to monitor the bridge dynamic movements [8]. Under the mode of the RTK, the reference station serves as a stationary checkpoint whose 3D coordinates have been previously determined by the conventional static GPS method and constantly records the

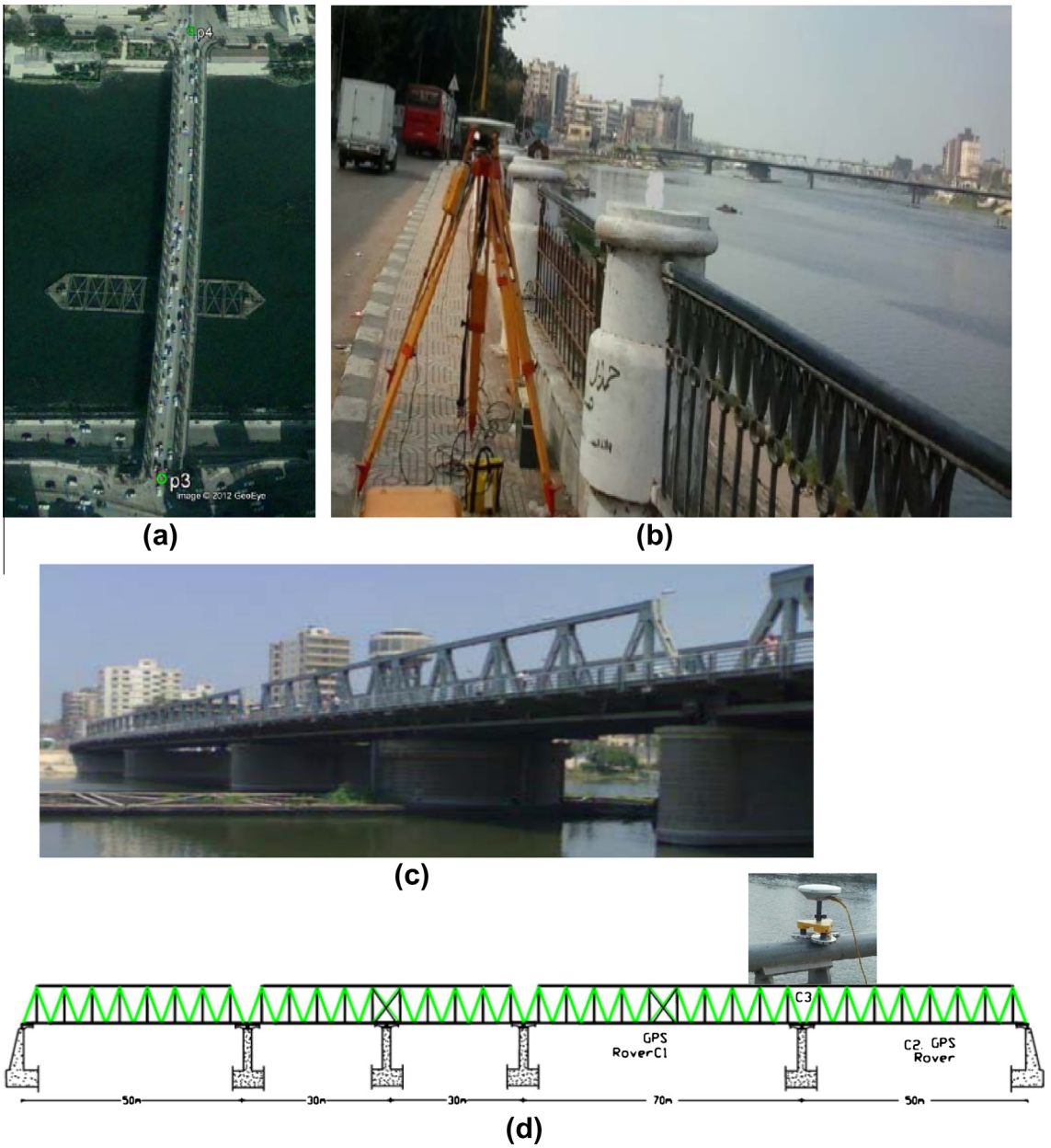

Fig. 1. (a) View of Google Earth bridge plan, (b) GPS-base station with side view of the bridge, (c) view of the bridge and (d) longitudinal section of the bridge with positions of the GPS rover.

difference between its known position and the position calculated from the satellite data [8,14]. The detected differences are indicative of the errors from the satellite hardware and more important, lower atmospheric delays with low time required to calculate a rover position. An ultra-high-frequency radio set is then used to send the errors to the rover. The rover, which is the GPS receiver whose position is being tracked, uses this error information to improve its accuracy. The clock offsets in the receivers, satellites and the atmospheric propagation delays can be ignored because the two receivers are in close proximity, which means that the errors are strongly correlated. In this study, the base GPS, rover GPS and radio unit (Fig. 1b and d) are used to collect raw data at rate of 1 Hz. The measuring condition was favorable and the receiver was free of any obstruction of 15° angle view of the horizon and at least four satellites were tracked continuously. The time observation for each rover point is one hour, approximately, to monitoring the bridge movement points on three dimensions and low frequency effects. The GPS base receiver, recording at 1 Hz, was placed approximately 576.0 m away from point C1 at stable ground, as shown in Fig. 1b.

The data collected were post-processed using GPS-Trimble software. The outputs of the GPS software was the time series of instantaneous Cartesian coordinates of

the rover receiver in the WGS84 coordinate system (N, E, H). A local Bridge Coordinate System (BCS) (X, Y, Z) is established to be used in the analysis and evaluation of the observed data. According to Fig. 1a, the coordinates in WGS84 are transformed into those in BCS by 2D similarity transformation (Eq. (1)). The azimuth (α) of the bridge is calculated as 2°18′36.71″. Herein, the X-data represents the displacement changes along the longitudinal of the bridge, the Y-data represents the displacement changes along the transverse of the bridge and the Z-data represents the relative displacement change a long the altitude direction of bridge.

$$\begin{bmatrix} X \\ Y \\ Z \end{bmatrix} = \begin{bmatrix} \cos\alpha & \sin\alpha & 0 \\ -\sin\alpha & \cos\alpha & 0 \\ 0 & 0 & 1 \end{bmatrix} \begin{bmatrix} N \\ E \\ H \end{bmatrix} \quad (1)$$

The receiver coordinates in the three dimensions (X, Y, Z) were transformed into time series of apparent (x, y, z) displacements (dx_i, dy_i, dz_i; $i = 1, 2, \ldots, n$) around a relative zero representing the equilibrium level of the monitored point. This similarity transformation was based on the following equation.

$$\begin{bmatrix} dx_i \\ dy_i \\ dz_i \end{bmatrix} = \begin{bmatrix} x_i \\ y_i \\ z_i \end{bmatrix} - \frac{1}{n} \sum \begin{bmatrix} x_i \\ y_i \\ z_i \end{bmatrix} \quad (2)$$

where n represents the total number of intervals recordings.

Fig. 2 shows the apparent of unfiltered displacement of the three dimensions of monitored points (C1, C2 and C3). The relative displacement of the three points is calculated based on Eq. (2) and the errors with more than three times the standard deviation of the relative movements are removed. Table 1 presents the statistical signals (mean, maximum, minimum and standard deviation; SD) of the displacements presented in Fig. 2.

From Fig. 2 and Table 1, the points' movements on the x-direction are lower than other directions at the three observed points; in addition the movements of point C2 are higher than other points in the three directions. Also, the movements of the three points are greater than the accuracy of GPS instruments used (Trimble 5700 GPS receiver), which is 1 cm + 1 ppm (length of base line) in horizontal direction and 2 cm + 1 ppm (length of base line) for the vertical direction [15]. From these results, it can be concluded that the points are moved in the three directions and the deformation in the z-direction is high at point C2 on bridge response. The sensitivity deformation of the z-direction is high with traffic load effect, so it is recommended to take the necessary precautions for the deck at point C2. In addition, the Multipath error is still one of the major sources of errors in GPS surveying.

Examining Fig. 2, at first glance, there is no evidence of dynamic displacement due to the dominating ambient noise. Therefore, it is necessary to de-noise the time series and extract the useful signal describing the dynamic displacement of the bridge. For this reason, the filtering produced with external constraints for analysis of the time series of apparent displacement defined by Eq. (1) is presented in the following sections.

3. De-noising of GPS displacement amplitude

The time series data shown in Fig. 2 are de-noised using a simple low-pass moving average filter with a step of 55 s and the output results are then smoothed [23,24]. Fig. 3 shows the original and the smoothed signals (red). The difference between the original and smoothed signals is presented in Table 1. From this figure, it can be seen that the errors of this receiver is high and the moving average filter is suitable to eliminate the errors and noise; whereas the accuracy of the smoothed signals is increased by about 15% than that of the original signals. The mean value of the bridge displacement (Table 1) is very low at the three points in the three dimensions. In addition, the remaining displacement amplitude is high at point C2. Also, the observed deformation changes in lateral and longitudinal directions are almost the same at points C1 and C2 (Fig. 3), whereas the movements at the three directions of point C3 are not the same. The displacements of point C3 reveal the movement of the cantilever handrail of the bridge. The temperature changes and wind speed at the observation time were about 3 °C and 18 km/h. Based on previous studies [19,25], these temperature changes and wind speed are ineffective on the bridge movement. Accordingly, the main source of the bridge deformation is the traffic loads.

4. Bridge dynamic analysis

Designing a proper digital filter for the extraction of structural dynamics is an important aspect of structural deformation analysis [23,24]. In this section, the bridge vibration is analyzed based on two steps [13,26]. The first step concerns computing the short-period component of the GPS observation signals and the second step deals with the spectral analysis of the low frequency displacement.

4.1. Short-period GPS observation component

A Hamming window-based Finite Impulse Response (FIR) filter is used in the design of a band-pass filter using pass-band and stop-band frequencies, pass-band ripple in decibels, filter order and window type as its input parameters to the filter [23,24,27]. FIR filter is a linear phase which is important in digital filter design whereas it results in a pure time delay with no amplitude distortion and the Hamming window is optimized to minimize the leakage of the signal energy to other frequencies [24]. As shown in Fig. 4, the frequency responses of a 100th order FIR type digital filter can be used to detect responding frequencies between 0.02 and 0.40 Hz. This filter is designed in Matlab with the following parameters: 100th-order; pass-band normalized frequency $0.04 \leqslant w_n \leqslant 0.8$; pass-band ripple zero dB and Hamming window of length 101. The short-period displacement components of the z-direction at the three points are shown in Fig. 5. It can be seen that the short-period contains the dynamic displacement of the vibration signals with high noise. Based on previous studies, this occurred due to white noise with Multipath and receiver errors [26–28]. Herein, the dynamic response of

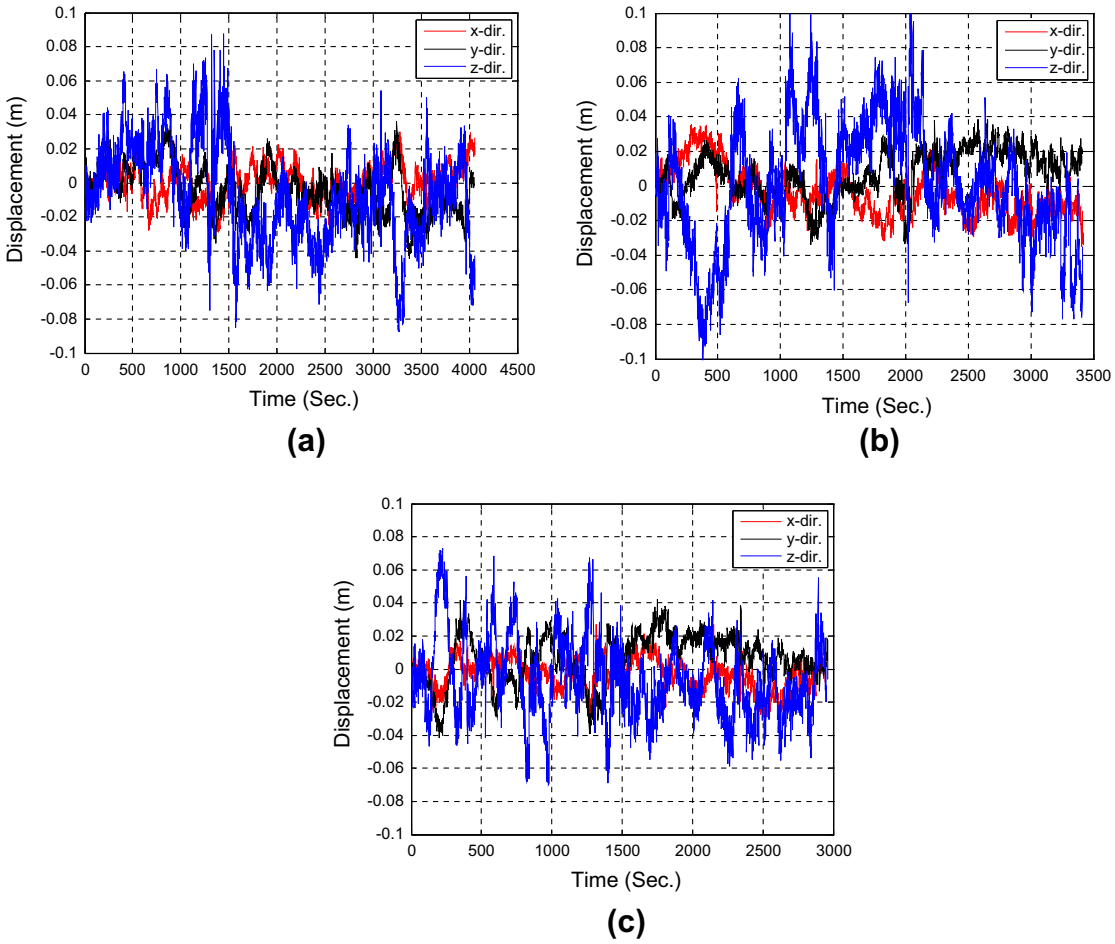

Fig. 2. GPS monitoring displacement of points: (a) C1, (b) C2 and (c) C3.

the bridge oscillations contains a handrail vibration effects which can be computed from the short-period using second level filter. The short-period components were filtered using a simple moving average filter over a 37 s period using the following equation.

$$y(j) = \frac{1}{k}\sum_{j-k}^{j} x(j) \tag{3}$$

where; $y(j)$ is the dynamic response of the structure at epoch j and k is the size of moving average window (this equates to 37 points at a data rate 1 Hz).

The dynamic displacement filtered from short-period component is, also, shown in Fig. 5. It can be seen that the errors of the GPS signals due to Multipath, receiver and white noise are very high with this receiver type. Also, some remnant noise still exists (Fig. 5b and f and Table 2) where the excitation period is well marked and is well distinct from the periods before and after second filter. Oluropo et al. [13], Meng [27] and Roberts et al. [28] used Choke ring antennas in order to mitigate some of the effects of multipath. In addition, the multi filter can eliminate some of the errors as shown in Fig. 4 and this result is cited in references [7,8,13,18,22,27,28]. The short-period and the dynamic displacement of the bridge oscillations at the three points are within +3 cm and +5 mm, respectively (Fig. 5a, c and e). The results of this analysis reveal that the dynamic behavior of the bridge is safe under the current loads.

4.2. Spectral analysis of the dynamic displacement

In this part, the Fast Fourier Transformation (FFT) is used to compute the low frequency effects of the dynamic displacement of the bridge. The dynamic amplitude spectral on the z-direction of the bridge monitored points is shown in Fig. 5. Table 2 summarizes the first five dynamic low-frequency modes response of the bridge. The multi filtering of the GPS signals displacement allows the appearance of the low-frequency modes of structures when comparing it with previous studies [19,29]. From Table 2, it can be seen that the five modes are appeared on the z-direction at the three points and in the x and y-directions at point C2 only. In addition, the values of the second mode to the fifth mode are close at the three monitored points whereas the first mode is different. Thus means that the first mode in the three dimensions at the three points are

Table 1
Movement of the monitored points before and after de-noising (units are in cm).

Monitoring Point	C1						C2						C3					
	x-Before	*x*-After	*y*-Before	*y*-After	*z*-Before	*z*-After	*x*-Before	*x*-After	*y*-Before	*y*-After	*z*-Before	*z*-After	*x*-Before	*x*-After	*y*-Before	*y*-After	*z*-Before	*z*-After
Mean	0.078	0.0012	−0.411	−0.0003	−0.616	0.0015	−0.336	−0.0027	0.680	0.0004	0.102	0.0003	−0.296	−0.0007	0.571	0.0013	−0.625	−0.0033
Max.	2.988	2.12	3.724	3.59	8.784	4.95	3.545	2.15	3.864	2.30	10.565	6.15	2.799	1.66	4.231	2.54	7.293	5.55
Min.	−3.066	−2.12	−4.437	−2.47	−8.749	−5.32	−3.633	−1.99	−3.431	−2.84	−10.219	−8.27	−2.882	−1.69	−4.274	−3.28	−7.013	−4.22
SD	1.020	0.84	1.468	1.12	2.915	2.31	1.362	0.94	1.297	1.02	3.505	3.17	0.943	0.74	1.473	1.25	2.433	1.80

due to the remaining noise of the GPS signals [26]. Also, the low frequency calculated for the three monitored points of the bridge are found to be approximately equal. The main reason for this is due to the fact that the observation time for the bridge (one hour) was lower than the time necessary for the determination of low-frequency changes in the bridge movements. However, it can be concluded that the low-frequency movements of the bridge could not be completed in the given observation time and the observation time should be longer than one hour. Based on the current study, the bridge dynamic modes are safe as per the presented frequencies.

5. System identification of bridge movement

In most practical applications, the system is not known and has to be estimated from the available information. This is called the identification problem. The identification method depends on the model used [14,30]. The three main choices in system identification are data, model class and criterion. In addition, system identification often involves several runs of the empirical cycle which consists of the specification of the problem, the estimation of a model by the criterion optimization, the validation of the resulting model and possible adjustments that may follow from this validation. In this section, the deformation identification for the *z*-direction of point C2 is studied and model identification is created based on a single-output movement of the bridge deck using Neural Network Auto-Regressive (NNAR).

In general, the Auto-Regressive (AR) structure [17,21,23,24] uses delayed inputs and outputs in order to determine a prediction of the output at one (or more) sample interval(s) in the future. It is presented in the form given by the following equation:

$$\tilde{y}(t) = \tilde{f}[x(t)] \tag{4}$$

where $\tilde{y}(t)$ represents the model prediction, $x(t)$ represents the regression vector of current and past inputs, outputs and additive pre-filtered noise and $\tilde{f}(.)$ is some function of $\underline{x}(t)$.

Parameter estimation of the linear AR models followed a standard minimization of the sum squared errors approach [21]. In the absence of noise, the model could be determined directly from linear algebra from very few data points, in a relatively trivial manner. In the AR structures, it is assumed that the noise is equivalent to pre-filtered white noise where the poles of the filter are identical to those of the resulting AR model. Practically, this means that iterations may be necessary to ensure that deviation from this assumption does not have a deleterious effect on the model predictions [17]. Assuming unit sampling interval, there is an output quantity or signal $y(t) = 1, 2, 3, \ldots, n$. Assuming that the signals are related by a linear system AR model, this is can be presented in the following form:

$$\tilde{y}(t) + y(t)(a_1 q^{-1} + a_2 q^{-2} + \ldots a_{\mathrm{na}} q^{-\mathrm{na}}) = e(t) \tag{5}$$

where $a_1, a_2, \ldots, a_{\mathrm{na}}$ are constant coefficients which form the parameters to be estimated; $\tilde{y}(t)$ is the one-step-ahead

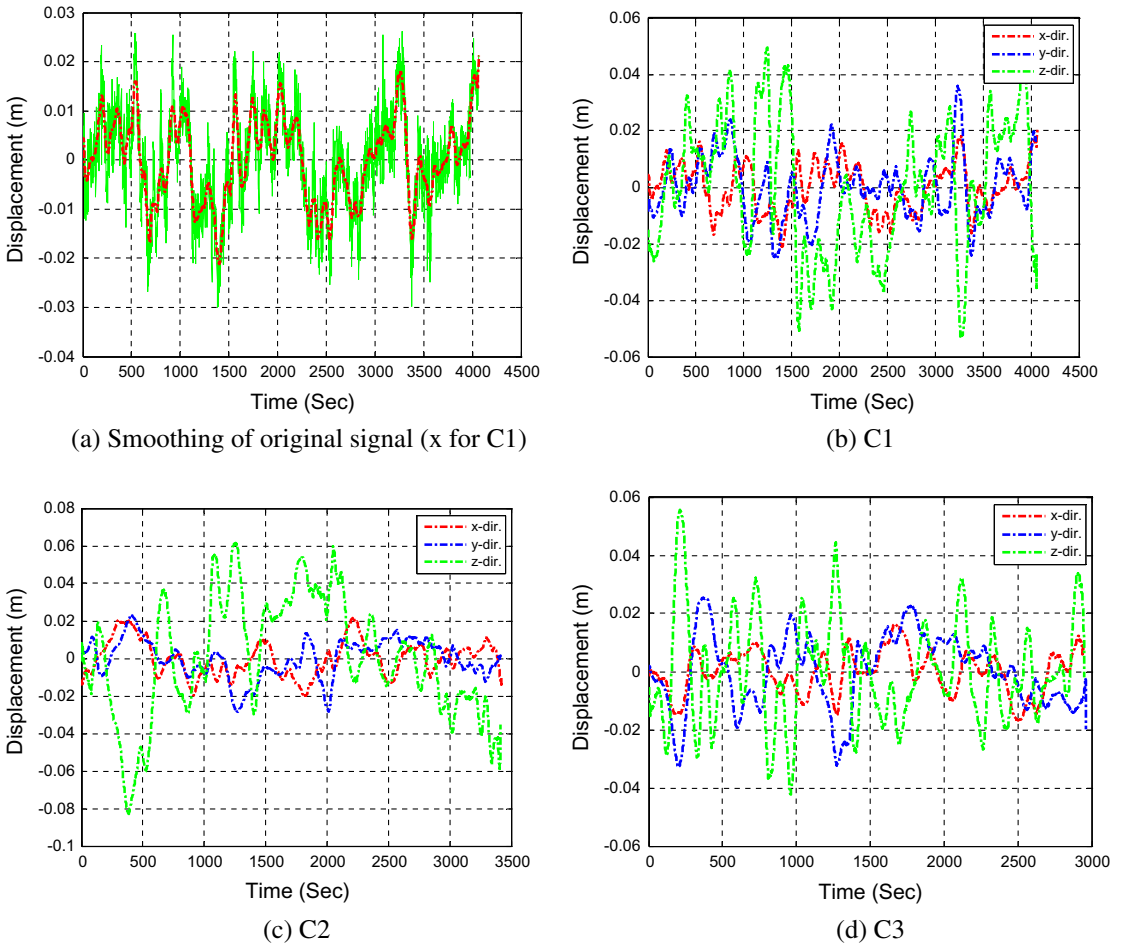

(a) Smoothing of original signal (x for C1)

(b) C1

(c) C2

(d) C3

Fig. 3. Smoothed GPS displacement signals of the monitored points.

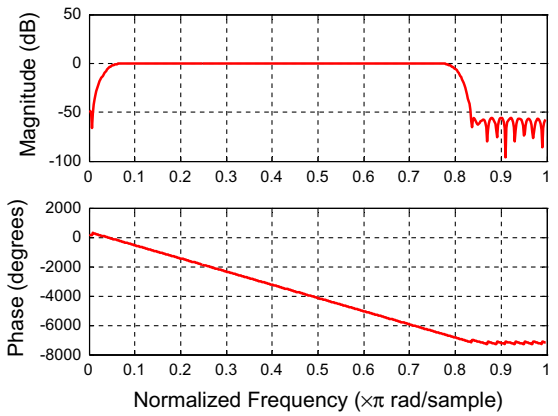

Fig. 4. The FIR digital band-pass filter of 100th order.

prediction of $y(t)$ the actual output; q^{-1}, q^{-2},...q^{-na} represent the delay operator, $e(t)$ is the additive noise, na length of the output regression vector.

In this paper, using Multilayer Perceptron (MLP) network to estimate the parameters and predict model output of Eq. (5). The MLP-networks considered here having only one hidden layer and only hyperbolic tangent and linear activation functions (f, F):

$$\tilde{y}_i(w,\ W) = F_i\left(\sum_{j=0}^{q} W_{ij} f_j\left(\sum_{l=1}^{m} w_{jl} z_l + w_{j0}\right) + W_{i0}\right) \tag{6}$$

where, $\tilde{y}_i(w, W)$ is the prediction of the model as a function of network weights; w_{j0} and W_{i0} are the bias parameters; m is the number of input units and q is the number of hidden units. The function $f(.)$ that is implemented in this paper is tangent function and $F(.)$ is linear function output. The weight (alternatively by the matrices w and W) are the adjustable parameters of the network; z_l represents the feature vector of length m, presented to the input of a feed forward neural network. In this case, a feed-forward neural network is used with an input layer of m nodes for $n = 1\ldots m$, one hidden layer and a single output layer. The input layer includes the input variables. The hidden layer consists of five hidden neurons or units placed in parallel. Each neuron in the hidden layer performs a weighted summation of the weights which then passes an activation function. The output layer of the neural network is formed by another weighted summation of the outputs of the neurons in the hidden layer [21]. The purpose of the neural

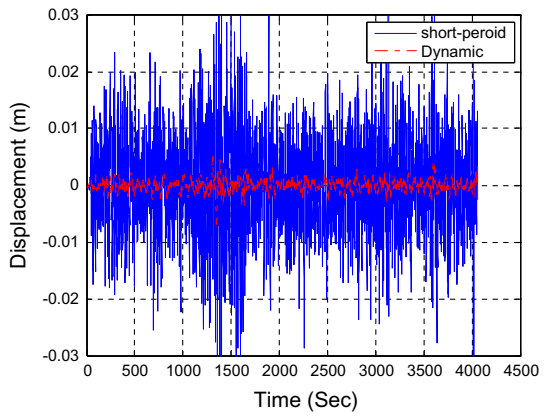

(a) Short-period and dynamic displacement of point C1

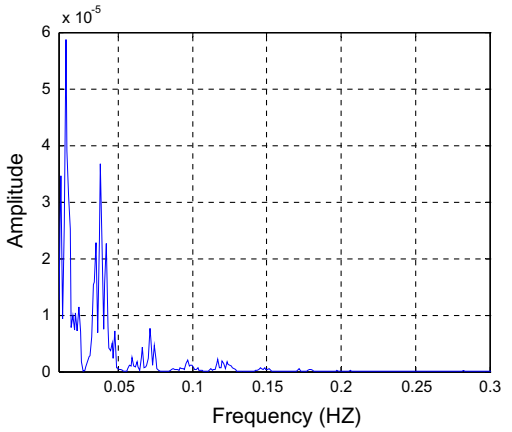

(b) Amplitude spectrum of point C1

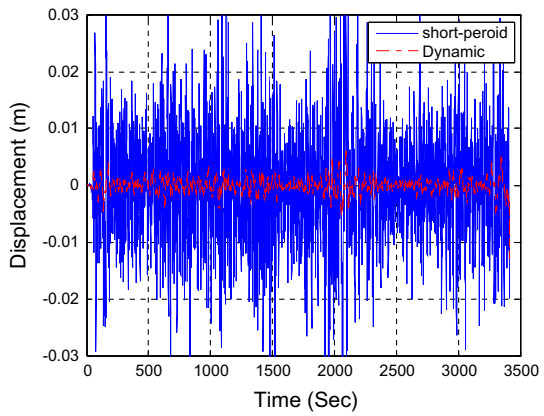

(c) Short-period and dynamic displacement of point C2

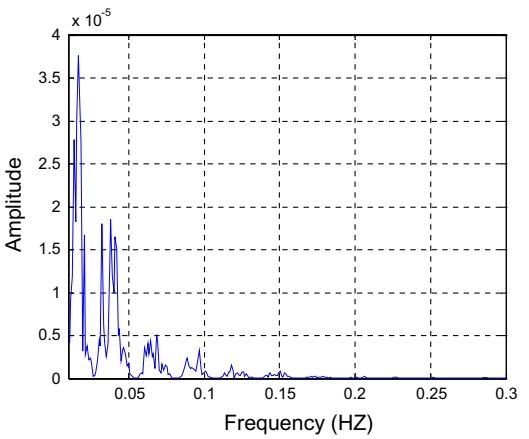

(d) Amplitude spectrum of point C2

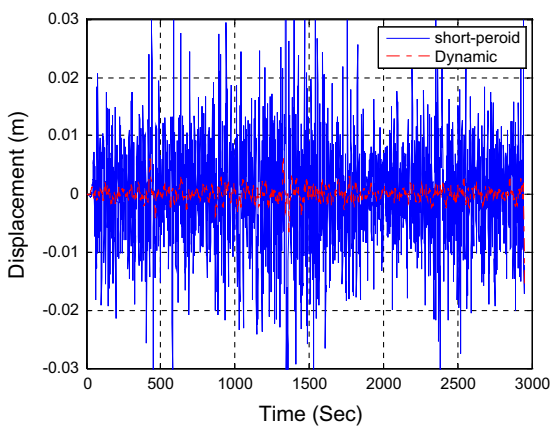

(e) Short-period and dynamic displacement of point C3

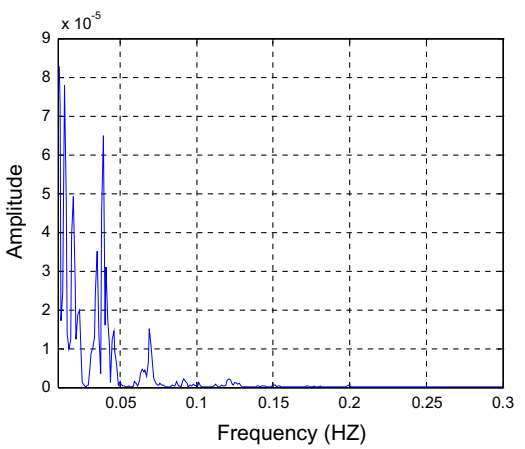

(f) Amplitude spectrum of point C3

Fig. 5. Short-period with dynamic displacement and amplitude spectrum in the *z*-direction.

network learning process is to apply corrective adjustments to the synaptic weight of neuron in order to make the output to come closer to the desired response in a step-by-step manner to satisfy the minimum loss function and the Akaike's Final Prediction Error (FPE). Finally, the following neural network regression model is proposed:

Table 2
The first five–frequency modes shape of the bridge movement (Hz).

Point	Frequency modes	x-Direction	y-Direction	z-Direction
C1	f1	0.0156	0.0137	0.0146
	f2	0.0381	0.0381	0.0381
	f3	0.0654	0.0664	0.0713
	f4	0.0957	0.0967	0.0967
	f5	–	–	0.123
C2	f1	0.0186	0.0166	0.0166
	f2	0.0391	0.0391	0.0381
	f3	0.0674	0.0654	0.0684
	f4	0.0967	0.0967	0.0967
	f5	0.125	0.1211	0.1182
C3	f1	0.0176	0.0127	0.0137
	f2	0.0391	0.0391	0.0391
	f3	0.0664	0.0693	0.0693
	f4	0.0947	0.0918	0.0918
	f5	–	–	0.1221

Table 3
Parameters of NNAR models of the deck displacements in *z*-direction. For point C2.

Model	λ_0	FPE (e^{-8})
NNAR(5)	1.5 e^{-5}	4.7
NNAR(10)	1.2 e^{-5}	4.6
NNAR(15)	1.9 e^{-6}	4.5
NNAR(20)	1.5 e^{-5}	4.5

$$\tilde{y}_i = \sum_{i=1}^{P} (\varphi_i y_{i-1} + b) w_{kj} \tag{7}$$

where φ_i are weights that defined or determined; $i = 1,2\ldots p$ is the number of lags as in the case of AR models, w_{kj} are the optimized weights from hidden to input layer and b is the bias which is a vector of ones as in the case of the ordinary least squares method. In addition, the following criteria can be used to evaluate and compare the quality of the model. The first: is the value of the loss function defined as:

$$\lambda_0 = \frac{1}{n}\sum_{t=1}^{n} e^2(t) \tag{8}$$

where $e(t)$ is an error value between the observed and the predicted model values ($e(t) = y(t) - \tilde{y}(t)$). The second criterion includes penalties for model complexity similar to the FPE criterion which is defined as:

$$\mathrm{FPE} = \lambda_0 \left(1 + \frac{2k}{n-k}\right) \tag{9}$$

where λ_0 is the loss function and k is the number of parameters in the model. The FPE represents a balance between the number of parameters and the explained variation. The third quality criterion for the model is provided by the Auto-Correlation Function (ACF) of the errors. The lag (m) Auto-Correlation (AC) is defined as:

$$\lambda_{(m)} = \frac{1}{n}\sum_{t=1}^{n} e(t-m)e(t) \tag{10}$$

Herein, the error is white noise; the AC $\lambda(m)$ is zero when k is nonzero. A large AC when k is nonzero indicates that the error is not zero-mean white noise and also implies that the model structure is not relevant to the model system or that there might be a need to increase the model order. In real applications, AC $\lambda(m)$ cannot be zero when m is nonzero because of limited length of observation points. If the value of AC falls within 95% of the confidence interval, the AC value is insignificant and this value is considered to be equal to zero [21].

The results of this model are shown in Table 3 and Fig. 6. The model evaluation criteria; loss function $\lambda_{(0)}$ and FPE values were calculated. The minimum $\lambda_{(0)}$ and FPE values were selected as the proper model to express the deck deflection (Table 3). The ACF and 95% confidence intervals of the residuals for the selected NNAR(na) model for *z*-direction are presented in Fig. 6b. In the definition of the Talkha bridge movements with NNAR model, time lags are taken into account as well as the previous input and output quantities. This type of model reflects the dynamic system as "systems that store energy and release it over a

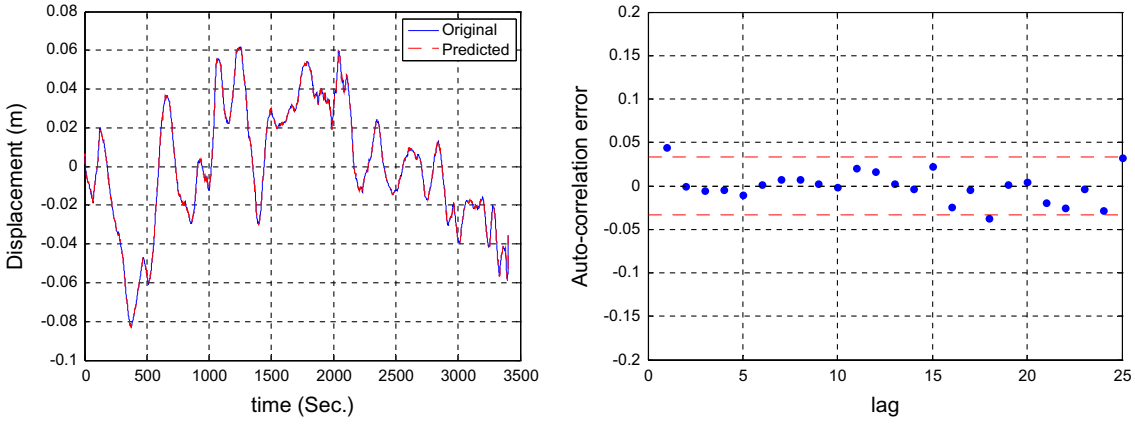

(a) AR(15) model with original signal (b) ACF and 95% confidence AR(15) model

Fig. 6. AR(15) model identification and ACF in *z*-direction for point C2.

time span". However, the bridge movement was modeled with NNAR model shown in Table 3 and Fig. 6a which have the capability of modeling dynamic response of the studied bridge. The results of the multiple regression analysis facilitated the definition of single output AR models of different orders and time lags. From Table 3, it can be concluded that the NNAR(15) model is suitable to predict the deck deflection. The movement output of the NNAR(15) model and filter observations of the bridge deck deflection at point C2 is presented in Fig. 5a. It is clearly seen that the model output is in conformity with the observations filter. ACF and 95% confidence intervals of the NNAR(15) model residuals is also presented in Fig. 6b. It can be concluded that no loss of information was observed since the residuals of this model stayed within the confidence interval of the autocorrelation function. The autoregressive models were, also, tried and it was concluded that they were harmonious with z-movement mode of different degrees as given in Table 3. Accordingly, the NNAR(15) model reflects the behavior of the bridge deck deflection at point C2 under effective loads and can be used to present more accurately movement of the bridge without any loss of information.

6. Conclusions

Talkha highway steel bridge is one of the two oldest steel bridges in Mansoura city. With the increasing of the traffic between Talkha and Mansoura cities, it becomes necessary to monitor this bridge periodically. In this study, RTK-GPS (1 Hz) is used to monitor and model the movement of the bridge deck. From this study, it could be concluded that.

The three monitoring points are moved in three directions and the deformation in the z-direction is high at point C2. So, it is recommended to take the necessary precautions of the bridge deck at point C2. In addition, the Multipath error is still one of the major sources of error in GPS surveying. It is also clear that some synthesis of this data is needed to make it meaningful. At first glance, the data provides no evidence of dynamic displacement due to the dominating ambient noise.

The moving average filter is suitable to smooth the high noise and errors of GPS observation signals; whereas the accuracy of the smoothed signals is increased by about 15% than that of the original signals. After signal smoothing, the displacement amplitude remains high at point C2. The observed deformation changes in the lateral and the longitudinal directions are almost the same at points C1 and C2; whereas at point C3, the movements of three directions are not the same. In addition, the movements of point C3 reveal the movement of cantilever handrail of the bridge. The temperature changes and wind speed at the time of the study were about 3 °C and 18 km/h which seems to be ineffective on the bridge movement; so the effective loads on the deformation of the bridge is the traffic loads.

The multi filter and FIR with moving average filter of short-period can be used to reveal the dynamic displacement of the bridge deck movement. The errors of the GPS signals due to Multipath, receiver and white noise are very high with receiver use. Also, the multi filter can be used to eliminate some of errors. The FFT is used to compute the frequency of the dynamic displacement of the bridge. The summarized first five dynamic frequency modes response of the bridge are presented. The multi filtering of the GPS signals displacement is used to show the frequency modes of the structure. In addition, the computed values from the second mode to the fifth modes are close at the three monitored points whereas the first mode is different due to the remaining noise of the GPS signals. In addition; it can be seen that the low-frequency movements of the bridge could not be completed in the given observation time and the observation time should be longer than one hour. The five dynamic modes of the bridge are safe based on these observations.

To identify the output movement of this bridge, a NNAR model is used. From the statistical analysis of the parameters and output residuals, it can be seen that the NNAR(15) model is suitable to predict the deck deflections. The movement output of the NNAR(15) is very conformed with the filter observations. ACF and 95% confidence intervals of the model residuals of NNAR(15) shows that no loss of information is observed since the residuals of this model stayed within confidence interval of the auto-correlation function. Herein, we can conclude that the NNAR(15) model reflects the behavior of the bridge deck deflection at point C2.

Acknowledgement

This research was supported by Mansoura University, Egypt.

References

[1] H. Sohn, C.R. Farrar, F.M. Hemez, D.D. Shunk, D.W. Stinemates, B.R. Nadler, J.J. Czarnecki, A Review of Structural Health Monitoring Literature form 1996–2001, Los Alamos National Laboratory report LA-13976-MS, 2004.
[2] C.R. Farrar, K. Worden, An introduction to structural health monitoring, Roy. Soc. London Trans. Series A 365 (1851) (2006) 303–315.
[3] J.P. Lynch, Y. Wang, K.-C. Lu, T.-C. Hou, C.-H. Loh, Post-seismic damage assessment of steel structures instrumented with self-interrogating wireless sensors, in: Proceedings of the 8th National Conference on Earthquake Engineering, San Francisco, CA, April 18–21, 2006.
[4] E. Figueiredo, G. Park, J. Figueiras, C. Farrar, K. Worden, Structural Health Monitoring Algorithm Comparisons Using Standard Data Sets, Report LA-14393, Los Alamos, USA, 2009.
[5] R. Guidorzi, R. Diversi, L. Vincenzi, C. Mazzotti, V. Simioli, Structural monitoring of the Tower of the Faculty of Engineering in Bologna using MEMS-based sensing, in: Proceedings of the 8th International Conference on Structural Dynamics, EURODYN 2011 Leuven, Belgium, 2011, pp. 4–6.
[6] J. Wenga, C. Loha, P.J. Lynchb, K. Lua, P. Linc, Y. Wangd, Output-only modal identification of a cable-stayed bridge using wireless monitoring systems, Eng. Struct. (30) (2008) 1820–1830.
[7] F. Moschas, S. Stiros, Measurement of the dynamic displacements and of the modal frequencies of a short-span pedestrian bridge using GPS and an accelerometer, Eng. Struct. J. 33 (2011) 10–17.
[8] S. Been, S. Hurlebaus, Y. Kang, A summary review of GPS technology for structural health monitoring, J. Struct. Eng. (2011), http://dx.doi.org/10.1061/(ASCE)ST.1943-541X.0000475.
[9] V. Zarikas, V. Gikas, C. Kitsos, Evaluation of the Optimal Design "Cosinor" Model for Enhancing the Potential of Robotic Theodolite Kinematic Observations, Measurement J. 43 (2010) 1416–1424.
[10] B. Riveiroa, H. González-Jorge, M. Varela, D.V. Jauregui, Validation of terrestrial laser scanning and photogrammetry techniques for the

measurement of vertical underclearance and beam geometry in structural inspection of bridges, Measurement J. 46 (1) (2013) 784–794.
[11] V. Gikas, Ambient vibration monitoring of slender structures by microwave interferometer remote sensing, J. Appl. Geod. 6 (3–4) (2012) 167–176.
[12] B.J. Costa, J.A. Figueiras, Fiber optic based monitoring system applied to a centenary metallic arch bridge: Design and installation, Eng. Struct. J. 44 (2012) 271–280.
[13] O. Oluropo, W. Gethin, J. Christopher, GPS monitoring of a steel box girder viaduct, Structure and Infrastructure Engineering: Maintenance, Management, Life-Cycle Design and Performance J., 2012, doi:10.1080/15732479.2012.692387.
[14] M. Kaloop, Structural Health Monitoring through Dynamic and Geometric Characteristics of Bridges Extracted from GPS Measurements. PhD-thesis, HIT, Harbin, China, 2010.
[15] User guide of Trimble (5700/5800 GPS Receiver).
[16] X. Meng, A.H. Dodson, G.W. Roberts, Detecting bridge dynamics with GPS and triaxial accelerometers, Eng. Struct. J. 29 (2007) 3178–3184.
[17] G. Premier, R. Dinsdale, A. Guwy, F. Hawkes, D. Hawkes, S. Wilcox, A comparison of the ability of black box and neural network models of ARX structure to represent a fluidized bed anaerobic digestion process, Wat. Res. 33 (4) (1999) 1027–1037.
[18] M.R. Taha, J. Lucero, Damage identification for structural health monitoring using fuzzy pattern recognition, Eng. Struct. 27 (12) (2005) 1774–1783.
[19] M. Kaloop, Bridge safety monitoring based-GPS technique: case study Zhujiang Huangpu Bridge, Smart Struct. Sys. 9 (6) (2012) 473–487.
[20] L. Li, H. Kuhlmann, Deformation detection in the GPS real-time series by the Multiple Kalman Filters Model, J. Surv. Eng. (136) (2010) 157–164.
[21] Norgaard M. Neural Network Based System Identification Toolbox, version2.Tech. Report. 00-E-891, Department of Automation, Technical Un. of Denmark, 2000.
[22] D. Jwo, C. Chang, C. Lin, Neural network aided adaptive Kalman Filtering for GPS applications, in: IEEE International Conference on Systems, Man and Cybernetics, 2004, pp. 3686–3691.
[23] H. Martin, Matlab Recipes for Earth Sciences, second ed., Springer, Berlin Heidelberg New York, 2007.
[24] Mathworks. Matlab, Release 12, The Mathworks, Inc., 2008.
[25] R. Kaloop, L. Hui, Tower bridge movement analysis with gps and accelerometer techniques: case study Yonghe tower bridge, Inf. Technol. J. 8 (2009) 1213–1220.
[26] F. Moschas, S. Stiros, Measurement of the dynamic displacements and of the modal frequencies of a short-span pedestrian bridge using GPS and an accelerometer, Eng. Struct. 33 (2001) 10–17.
[27] X. Meng, Real-time deformation monitoring of bridges using GPS/Accelerometers. PhD Thesis, Institute of Engineering Surveying and Space Geodesy, the Nottingham University, UK, 2002.
[28] G.W. Roberts, X. Meng, A.H. Dodson, E. Cosser, Multipath mitigation for bridge deformation monitoring, J. Glob. Position. Sys. 1 (2002) 25–33.
[29] M. Kaloop, H. Li, Monitoring of bridges deformation using GPS technique, KSCE J. Civil Eng. 13 (6) (2009) 423–431.
[30] G.F. Sirca, H. Adeli, System identification in structural engineering, Sci. Iran. A. 19 (6) (2012) 1355–1364.